Enthalpy of Formation of Calcium and Magnesium Oxide obtained by Knudsen Effusion Mass Spectrometry

Alexander Halwax [a, c], Dmitry Sergeev [b], Michael Müller [b], Johannes Schenk [a, c]

[a] K1-MET GmbH, Stahlstraße 14, 4020 Linz, Austria; alexander.halwax@k1-met.com

[b] IEK-2, Forschungszentrum Jülich GmbH, Jülich, Germany, d.sergeev@fz-juelich.de, mic.mueller@fz-juelich.de

[c] Department of Metallurgy, Chair of Ferrous Metallurgy, Montanuniversitaet Leoben,Franz-Josef Str. 18, 8700 Leoben, Austria, johannes.schenk@unileoben.ac.at

Abstract

Calcium and magnesium oxide are important components of metallurgical slag systems. However, the literature values for the standard enthalpy of formation $\Delta_f H^\circ_{298}$ of both oxides exhibit large variations in some cases. Since $\Delta_f H^\circ_{298}$ is crucial for the modeling and prediction of equilibrium states and, thus, also for process optimization; it was determined by Knudsen effusion mass spectrometry (KEMS). Pure CaO, as well as MgO, were investigated in an iridium Knudsen cell. For this purpose, the intensities of the main species present in the gas phase were recorded in a temperature range between 1825 to 2125 and 1675 to 2075 K, respectively, and their partial pressures were obtained. It was observed that CaO and MgO evaporated congruently with the main species in the gas phase, Ca, Mg, O, and O_2. The experimental vapor pressures of the gas species in the study of MgO are in good agreement with the calculated values using FactSage™ 7.3 and the FactPS database. While those for the evaporation of CaO show significant differences. These calculations are based on available thermodynamic information, including the Gibbs energy functions of CaO(s), Ca(g), MgO(s), Mg(g), O(g), and O_2(g). After calculating the partial pressures and equilibrium constants of reactions, an average formation enthalpy of $\Delta_f H^\circ_{298}$= -624.5±3.5 kJ/mol for CaO(s) and $\Delta_f H^\circ_{298}$= -598±10 kJ/mol for MgO(s) based on the third law method of thermodynamics were obtained. The deviation of $\Delta_f H^\circ_{298}$ for MgO from the previous literature values can be attributed to the use of different ionization cross sections, temperature calibration, and variation of tabulated Gibbs energy functions.

Keywords

Standard enthalpy of formation; Calcium oxide, Magnesium oxide; Knudsen effusion mass spectrometry

1. Introduction

Calcium and magnesium oxide are two of the most important constituents of metallurgical slags and fluxes. Therefore, their thermodynamic properties are essential for the prediction of equilibrium states in pyrometallurgical processes. The standard free energy of formation of CaO and MgO is one of the key parameters for the modeling of phase diagrams of multioxide systems, which are of interest for the estimation of optimal process conditions in high-temperature processes. The values given in the literature for the standard enthalpy of formation $\Delta_f H^\circ_{298}$ of CaO and MgO, which are used for the calculation of the standard free energy of formation, are mainly based on bomb and solution calorimetry. The NIST-JANAF tables are commonly used as a work of reference for thermodynamic quantities [1]. For example, the data listed there serves as one of the inputs for the FactPS database. These tables include thermodynamic properties of single-phase substances in the crystalline, liquid, and ideal gas states over a wide temperature range. They also include some tables for multiphase substances. Specified properties are heat capacity, entropy, Gibbs energy function, enthalpy increment, enthalpy of formation, Gibbs energy of formation, and the logarithm of the equilibrium constant corresponding to the formation of any compound from the elements in their standard reference states. All relevant input data are reported for every table, and a critical review of the literature on which these values are based is included. [1]–[8]

However, significantly different values for the standard enthalpy of formation of CaO $\Delta_f H^\circ_{298}$ can be found in the literature. For example, Gourishankar et al. in [9] determined a value of -602 kJ/mol (third law analysis [1],[10]) or -595 kJ/mol (second law analysis [1],[10]) by free-evaporation experiments. The value resulting from the third law analysis differs greatly from the -635.089 kJ/mol (third law analysis) given in the NIST-JANAF tables [1], which is based on bomb calorimetry experiments by Huber and Holley in [11] and the value of acid solution calorimetry given by Rossini et al. in [12]. Wakasugi and Sano concluded in [3] that $\Delta_f H^\circ_{298}$ is -610 kJ/mol (third law analysis) by equilibrium experiments between silver and a CaO-saturated slag. Liang et al. in [4] obtained a value of -634 kJ/mol for $\Delta_f H^\circ_{298}$ by a critical review of the experimental data, which serve as the basis for reference works and tables such as the NIST-JANAF data.

Somewhat similar differences can be found for the enthalpy of formation of MgO $\Delta_f H^\circ_{298}$. Thus, in the NIST-JANAF tables [1], a value of -601.241 kJ/mol is found. This value is based on the bomb calorimetry measurements of Holley and Huber [13] and the HCl solution calorimetry measurement of Shomate and Huffman [14]. Gourishankar et al. in [9] determined by free evaporation experiments $\Delta_f H^\circ_{298}$, which lies at -635 kJ/mol (third law method) and -643 kJ/mol (second law method), respectively. Using Knudsen cell mass spectrometry, Altman determined a $\Delta_f H^\circ_{298}$ of -572.13 kJ/mol in [15]. Liang et al. in [4] recalculated $\Delta_f H^\circ_{298}$ with a value of -601.60 kJ/mol by critically reviewing experimental data.

A summary of all literature values can be found in Table 4.

Such discrepancies in the enthalpy of formation have a significant influence on the calculated vapor pressures of the different species in equilibrium with the pure substance, which are based on these values. The impact of the formation enthalpy on the calculated vapor pressures of Ca, O, O_2 and Mg as a function of temperature are shown in Figure 1 to Figure 6. These calculations were performed using FactSage™ 7.3. Figure 1 to Figure 3 show the resulting vapor pressures at equilibrium with CaO. Figure 4 to Figure 6 the calculated vapor pressures in equilibrium with MgO. Since the values of the enthalpies of formation of Liang et al. [4] are very similar to those given in the NIST-JANAF tables [1], the different species have nearly identical vapor pressures.

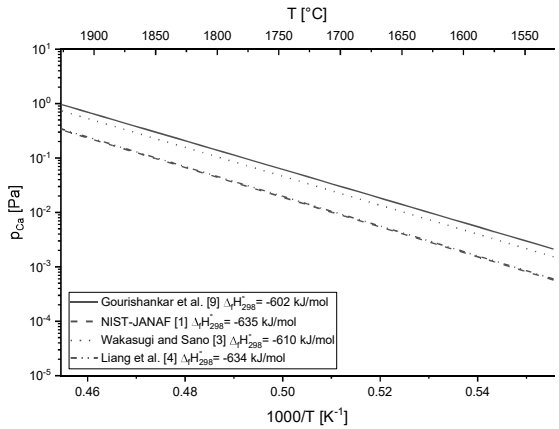

Figure 1: Influence of formation enthalpy of CaO on vapor pressure of Ca

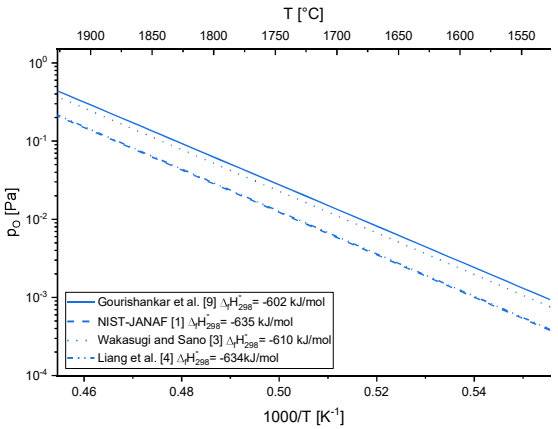

Figure 2: Influence of formation enthalpy of CaO on vapor pressure of O

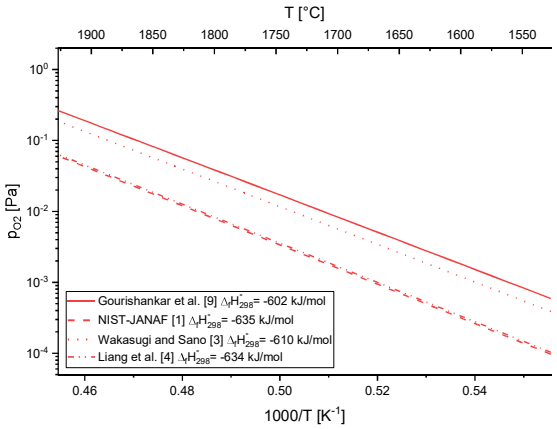

Figure 3: Influence of formation enthalpy of CaO on vapor pressure of O_2

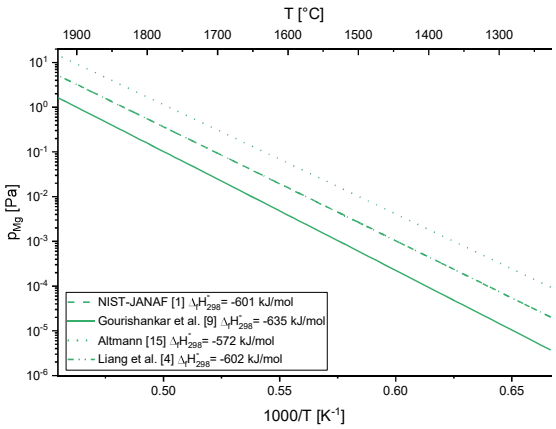

Figure 4: Influence of formation enthalpy of MgO on vapor pressure of Mg

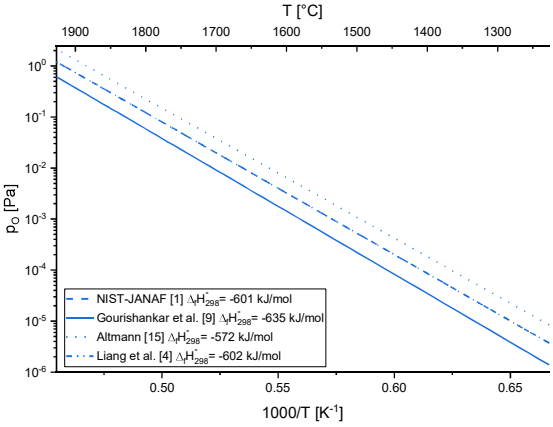

Figure 5: Influence of formation enthalpy of MgO on vapor pressure of O

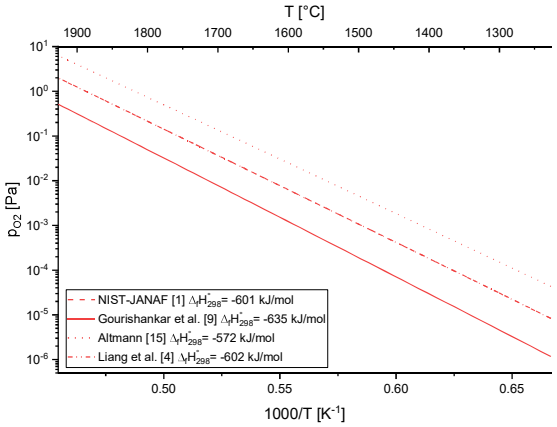

Figure 6: Influence of formation enthalpy of MgO on vapor pressure of O_2

The use of both reliable thermodynamic data and proper thermodynamic instruments enables thermochemical calculations to identify and predict thermodynamic properties as a function of composition, temperature, and pressure. A consistent data set of thermodynamic functions of condensed phases and all gaseous species is essential for the calculation of gas phase composition as well as vapor pressure over oxides. The calculation of equilibrium states is performed using the Gibbs energy minimization approach [16], which is implemented in commercial software (FactSage^{TM} [17], Thermo-Calc [18], etc.). This procedure gives the possibility to estimate the concentrations of all potential species according to the calculated Gibbs energies of all components in case the corresponding thermodynamic data are available and trusted. Such thermodynamic calculations also allow the prediction of all potential reaction products, considering all reactions between condensed and gaseous phases (recombination, melting, evaporation, decomposition, sublimation, etc.) at the same time [19].

Due to the significant differences in literature data for $\Delta_f H^{\circ}_{298,CaO}$ and $\Delta_f H^{\circ}_{298,MgO}$ and the fact that information about the thermodynamic data can be received directly by measurement of vapor pressure under equilibrium conditions, the evaporation behavior of CaO and MgO was investigated in view of planned activity determinations in metallurgical slags by KEMS at the Forschungszentrum Jülich. [20]

2. Principle of Knudsen effusion mass spectrometry

Knudsen effusion mass spectrometry (KEMS) is an experimental method that offers the most accurate equilibrium evaporation studies and provides direct information on thermodynamic properties. Since this method has rarely been used for metallurgical research purposes, this section will provide a brief insight into the background of KEMS. [20]–[22]

The setup of a Knudsen effusion mass spectrometer consists of two vacuum chambers that can be separated from each other, a Knudsen cell, a pyrometer, an electron impact ion source, a single-focusing magnetic type sector field mass spectrometer and a collector arrangement of the secondary electron multiplier. The shutter serves to separate the two vacuum chambers (mass spectrometer and Knudsen cell chamber) and to shield the ion source from the molecular beam emitted out of the Knudsen cell. A condensed sample is loaded into the Knudsen cell and kept at constant temperature and ultra-high vacuum until chemical and thermal equilibrium between condensed and gas phases is reached. An orifice ($0.3 - 0.5$ mm) in the lid of the cell allows a small fraction of the gas phase to effuse, forming a molecular beam, representing the equilibrium gas phase in the cell. The small number of effusing

molecules practically do not disturb the equilibrium inside the cell. This molecular beam enters the ion source, where the individual species in the gas phase are ionized by electron impact. The resulting ions are focused through a series of collimating lenses, and an applied accelerating potential on the way to the entrance slit of the mass analyzer increases the kinetic energy of these. Electric and magnetic fields oriented perpendicular to each other influence the path of the ions through the sector field analyzer by their combined effect. The dynamic change of the electric field strength causes a separation of the different ions according to their mass-to-charge ratio. Afterwards they hit the first dynode of the multiplier, where they cause a secondary emission of electrons. A cascade of plates, with increasing potential difference amplifies the secondary electrons. A potential drop converts the counted ions into an intensity signal. [21]–[25]

2.1. Partial pressure

From the ion intensities measured using the KEMS, the partial pressure p_i of the respective species can be calculated using Equation (1) [20],[21],[24],[25],[27]–[32]:

$$p_i = \frac{k I_i T f_i}{n_i \gamma_i \sigma_i} \tag{1}$$

Where k is the pressure calibration factor or the instrument sensitivity factor, I_i represents the measured ion intensity of the respective ion at the temperature T, T denotes the temperature in Kelvin in the Knudsen cell and f_i is the fragmentation correction factor. f_i is the ratio of M^+ to $\sum M^+$. n_i expresses the isotopic abundance of species i, γ_i is the multiplier factor of species i and σ_i stands for the ionization cross-section of the species i. γ_i describes a value of the secondary electron emission from the first dynode of a multiplier that depends on the mass and molecular structure and is set to 1 for the two elements because an ion counting system was applied in the KEMS. Therefore, the error of γ_i is considered to be 0. k is the sensitivity factor of the instrument and characterizes the transmission of ions by the mass spectrometer and enables the determination of absolute partial pressures. The determination of k is based on vaporization experiments of a substance with a well-known partial pressure (usually pure metals, e.g., Ag, Au, Ni, Pt [10]) in a well-defined temperature range (preferably around the melting point). The partial pressure thus obtained is compared with literature values, and consequently, the calibration factor can be determined. The intensity I_i correlates to the frequency of a certain ion in the molecular beam effusing from the Knudsen cell. The measured value from the ion counter can be directly applied to Equation (1). The isotopic abundance n_i is calculated as the isotopic abundance of the measured mass in relation to the total mass and quantities. Note that the error of the

isotopic abundances is negligible for our needs. The ionization cross-section σ_i of a species describes the probability that the initial molecule or atom of this species will be ionized by electron impact at a certain ionization energy. [10],[20],[21],[23],[24],[32]

2.2. Thermodynamic properties

The reactions investigated with KEMS are, for example, dissociation and sublimation reactions [23],[27]:

$$AB(g) \rightleftharpoons A(g) + B(g) \tag{2}$$

$$AB(s) \rightleftharpoons A(g) + B(s) \tag{3}$$

$$A(s) \rightleftharpoons A(g) \tag{4}$$

To determine the thermodynamic properties of condensed phases, incongruent and congruent vaporization processes, such as reactions (3) and (4), are investigated. With knowledge about the partial pressures of the individual species in the gas phase, the equilibrium constants K_P of these reactions can be determined using Equation (5) [10],[20],[23],[27]:

$$K_P = \Pi \left(\frac{p_i}{p^\circ}\right)^{\nu_i} \tag{5}$$

Where ν_i is the stoichiometric coefficient of components in the reaction equation. The partial pressure for standard conditions according to the Clausius-Clapeyron equation is set to conditions at T = 298 K and p = 1 atm = 101325 Pa = p°. [10],[20],[23],[27]

The change in enthalpy associated with the reaction can be calculated using either the second or third law method. The second law method is based on the van't Hoff or Clausius-Clapeyron equation (Equation (6)) and allows the determination of the enthalpy change ($\Delta_r H_T^\circ$) of the reaction at the mean temperature of the experiment [1],[10],[21],[23]–[25],[29],[33]–[36]:

$$\frac{dlnK_p}{d(1/T)} = -\frac{\Delta_r H_T^\circ}{R} \tag{6}$$

where R is the gas constant (8.314 J/mol·K). The standard Gibbs energy can be defined on the basis of the equilibrium constant [1],[20],[21],[25],[35],[37]:

$$\Delta G_{(T)}^\circ = -RTlnK_p = \Delta_r H_T^\circ - T\Delta_r S_T^\circ \tag{7}$$

The rearrangement of Equation (7) enables a linear representation in an Arrhenius plot (lnK_p versus $1/T$) and links the equilibrium constant, the enthalpy and the entropy of the reaction (Equation (8)) [10],[20],[21],[24]:

$$lnK_p = -\frac{\Delta_r H_T^\circ}{R}\frac{1}{T} + \frac{\Delta_r S_T^\circ}{R} = -A\frac{1}{T} + B \tag{8}$$

This allows the analysis of the regression coefficient A and the intercept B and, thus, the evaluation of the enthalpy and entropy of the reaction at the mean temperature of the measurement. To recalculate the enthalpy of the mean temperature of the measurement to the standard temperature (typically 298 K), enthalpy increments $H(T) - H(298)$ have to be used. These can be found in typical reference works, for example, in [8],[38] and [1]. [1],[10],[21],[24],[32],[36]

As already mentioned, the reaction enthalpy at standard temperature $\Delta_r H_{298}^\circ$ of the investigated reaction can also be obtained by the third law method. It is based on the known absolute value of the equilibrium constant. Thus, the enthalpy of the reaction of each data point can be calculated if the change in Gibbs energy function is known. According to Equation (9) [1],[10],[23],[25],[34],[36],[37]:

$$\Delta_r H_{298,3rd}^\circ = -T\left[RlnK_p + \Delta_r gef_T^\circ\right] \tag{9}$$

$\Delta_r gef_T^\circ$ is the change of Gibbs energy function for the considered reaction. The change in Gibbs energy function must be obtained from the Gibbs energy functions gef_T°, according to the stoichiometry of the individual species at the measurement temperature. As shown in Equation (10). [32]

$$\Delta_r gef_T^\circ = \sum gef_T^\circ\,(products) - \sum gef_T^\circ\,(reactants) \tag{10}$$

gef_T° is calculated as follows (Equation (11)) [1],[32]:

$$gef_T^\circ = \frac{H_T^\circ - H_{298}^\circ}{T} - S_T^\circ \tag{11}$$

The advantage of the second law method compared to the third law method is the fact that because of the proportionality of $I_i T$ and p_i, the representation of $\ln(I_i T)$ over $1/T$ yields a linear plot where the slope is equal to $\frac{\Delta_r H_{Tm}^\circ}{R}$, which eliminates the need to calculate the absolute values of the vapor pressures. [23],[25],[34]

Data analysis by the third law method is generally considered to be of higher quality than analysis by the second law method. [1],[9],[37]

3. Experimental

The vaporization studies of pure CaO (Thermo Scientific™, 99.998%) and pure MgO (ROTI®METIC 99.999%) were carried out at the Forschungszentrum Jülich GmbH using a Finnigan MAT 271 (Finnigan MAT, Bremen, Germany) 90 ° magnetic sector-field mass spectrometer. To prevent reactions between the Knudsen cell and the sample, an iridium cell was used. The selection of the correct cell material is of great importance. Indeed, any reaction of the sample material with the cell would reduce the activity of the starting oxide, lowering the partial pressures of the gaseous products. Therefore, iridium was considered as a suitable cell material. The orifice in the lid of the cell had a diameter of 0.3 mm. The cell itself was placed in a molybdenum container, which had a hole at the bottom for temperature measurement, using an optical pyrometer. This cavity in the Knudsen cell array has geometric properties such that the emitted light approximates the behavior of a black body. To avoid high radiation losses, thermal isolation of the Knudsen cell was achieved by tantalum radiation shields during the measurements. The cell was heated by radiation and electron bombardment from a hot tungsten wire. Temperature adjustment was performed by a type K thermocouple and measured by an Impac IGA 12 optical pyrometer. The temperature is determined through a sighting hole aimed at the black body hole in the molybdenum container. Any discrepancies between the temperature measured by the pyrometer in the cavity and the actual temperature in the cell are corrected by measuring standards with known melting points. However, since only one Knudsen cell can be loaded at a time, the orientation may change as samples are replaced. Thermal conditions may therefore vary slightly depending on Knudsen cell placement, heat shield assembly, or Knudsen cell positioning, which would have a small but significant effect on the derived thermodynamic quantities. Therefore, a systematic error of ±5 K is estimated. Ions were detected using a continuous dynode multiplier linked to an ion counter. Ionization of the species in the vapor phase was achieved by applying an electron energy of 70 eV and an emission current of 0.2 mA. The accelerating voltage of the ions has been 8 kV.

For the calibration of the optical pyrometer and to determine the instrument sensitivity factor k, evaporation experiments were carried out with a pure nickel standard. Therefore, the change of the vapor pressure of Ni was recorded in a temperature range from about 1650 to 1800 K.

For calcium and magnesium oxide measurements, approximately 50 mg of the pure CaO or MgO powder was loaded into the iridium Knudsen cell. Table 1 lists the masses of the initial weights and the masses of the samples determined by differential weighing after the experiments.

Table 1: Initial sample masses and sample masses after the experiment

Measurement	Initial mass CaO [mg]	Mass after experiment CaO [mg]	Initial mass MgO [mg]	Mass after experiment CaO [mg]
1st measurement	53.93	45.06	53.67	49.25
2nd measurement	49.51	45.72	51.58	48.28

The cell was then placed in the Knudsen cell chamber. The chamber was closed and evacuated with a turbomolecular pump. As soon as the pressure decreased below 10^{-5} mbar, heating could be started. The cell was heated up to a temperature of approximately 775 K by radiation. After reaching this temperature, the heating system automatically switched to heating with electron bombardment. To check the presence of possible species in the vapor phase above the oxide sample, mass scans from mass 10 to 100 were performed at different increasing temperatures. Once a sufficiently high signal of $^{40}Ca^+$ or $^{24}Mg^+$ ions was detected, the cell position was adjusted to optimize the observed signal. For CaO, these mass scans detected $^{40}Ca^+$, $^{16}O^+$ and $^{16}O_2^+$ as the main ions. For MgO, $^{24}Mg^+$, $^{16}O^+$ and $^{16}O_2^+$ were detected as the main ions. Isothermal measurements were performed to determine the necessary duration required to reach equilibrium and to verify the stability of the vapor pressures. This was done by keeping the CaO sample at an average of 2077±5 K for 19 hours and measuring the intensity of $^{40}Ca^+$, $^{16}O^+$ and $^{16}O_2^+$ every hour. The same was done for the MgO sample, which was kept at an average of 1926±5 K for 15 hours and the intensities of the $^{24}Mg^+$, $^{16}O^+$ and $^{16}O_2^+$ ions were measured hourly. The polythermal measurements were carried out according to a predefined temperature program. Each temperature was held for 250 seconds before measuring ion intensity to ensure that equilibrium in the cell had been established. Measurements at each temperature step were taken first with an open and then with a closed shutter. This is necessary to be able to remove the background signal from the actual intensity of the species. The temperature steps between measurements were 10 K, and the heating rate was 10 K/min. The temperature range of those measurements were from ~1825 to ~2125 K for CaO and ~1675 to ~2075 K for MgO. The polythermal measurements were performed twice to verify the results reproducibility.

4. Results and discussion

4.1. Calibration

From the calibration measurements around the melting point of the pure Nickel standard and the comparison of the recorded ion intensity of $^{58}Ni^{+}$ and the partial pressure of Ni at the melting point (FactPS database), a pressure calibration factor of $7.6414 \cdot 10^{-9}$ was determined. The enthalpy of sublimation ΔH_{sub} of Ni at the mean temperature of the measurements was determined using the second law method. The result was an enthalpy of 422±4 kJ/mol at a temperature of 1727 K. Table 2 shows the comparison with previous literature values as well as the calculation by FactSage™ using the FactPS database. The experimentally determined value is within the ± 5 kJ/mol range with literature values, which is commonly acceptable [21].

Table 2: Enthalpy of sublimation of pure Ni

Source	ΔH_{sub} [kJ/mol]
This study	422±4
NIST JANAF tables [1]	418±8.4
Alcock et al. [39]	421±5
FactSage™	417

4.2. Isothermal measurement

Using Equation (1), the intensities of the respective species were converted into their partial pressures. The used ionization cross sections (σ_i) at an electron ionization energy of 70 eV as well as the isotopic abundance (n_i) of the different elements were taken from [40] and [41], respectively. In the case of O_2, the cross-section was calculated using Equation (12), which is valid for the calculation of the cross-section of molecules [19]. All used values are listed in Table 3. The ionization cross-sections used could be a possible source of error. There are different calculation approaches ([42]–[44]) and experimental determinations ([45]) of these cross sections. [19],[32]

$$\sigma_{mol} = 0.75 \sum_i \sigma_{at}(i) \tag{12}$$

Table 3. Ionization cross sections and isotopic distribution used for vapor pressure determination

Species/Isotope	σ_i [10^{-16} cm^2]	n_i
^{40}Ca	9.0534	0.96941
^{16}O	1.2677	0.99757

Species/Isotope	σ_i [10^{-16} cm^2]	n_i
$^{16}O_2$	1.9016	0.99515
^{24}Mg	4.6574	0.78990

The isothermal measurements of both CaO and MgO show a rapid setting of the equilibrium state. In the case of CaO, the equilibrium state (ignoring the runaways at nine hours) can be observed after only one hour. In the case of MgO, the Mg vapor pressure drops slightly over the first four hours of the measurement, but stabilizes after that, indicating that the equilibrium state has been reached. The results can be seen in Figure 7. The pressures calculated by FactSage™ 7.3 using the FactPS database are also plotted in the diagram in addition to the vapor pressures determined by KEMS. The calculations using FactSage™ 7.3 were performed at the mean temperatures 2077 and 1926 K, respectively, at a total pressure of 101325 Pa. The equilibrium partial pressures of all species in the gas phase were obtained, taking all possible reaction products into account. During the isothermal measurement of CaO, the average ratio of $\frac{p_{Ca}}{p_{Ca}\,FactSage}$ is approximately 2, $\frac{p_O}{p_O\,FactSage}$ almost 3, and $\frac{p_{O_2}}{p_{O_2}\,FactSage}$ about 2.5. The values of the first measurement as well as the values of the outliers at nine hours, were excluded. These results suggest that the thermodynamic properties of CaO stored in the databases used show a deviation from reality. The ratios $\frac{p_{Mg}}{p_{Mg}\,FactSage}$, $\frac{p_O}{p_O\,FactSage}$ and $\frac{p_{O_2}}{p_{O_2}\,FactSage}$ during the isothermal measurement of MgO show average values of 1, 2.2 and 1.5, respectively, after reaching the equilibrium state at 4 hours. This suggests that the thermodynamic functions for MgO in the databases are relevant to the actual measured values.

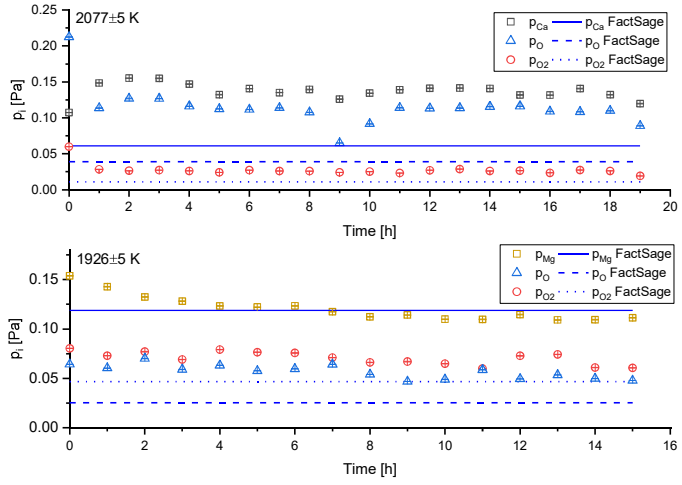

Figure 7: Isothermal measurement of CaO and MgO

A possible source of error in the measurements is the presence of oxygen in the residual gas within the KEMS system. This, in turn, leads to an error in the measured signal for $^{16}O^{+}$ and $^{16}O_2^{+}$. Furthermore, there is no condensation of oxygen in the molecular beam at the shutter surface. Which will result in an inaccurate signal of $^{16}O^{+}$ and $^{16}O_2^{+}$. In addition to the possible inaccuracy of the measurement results due to the presence of residual gas in the system, the fragmentation of O_2 can also cause the formation of $^{16}O^{+}$, which may result in a deviation of the measured ion intensity. [31]

4.3. Polythermal measurement

Similar to the isothermal measurement, the measured ion intensities were also converted into partial pressures for the polythermal measurement using Equation (1) and the parameters from Table 3. The determined pressures of the respective species are shown as an Arrhenius plot in Figure 9 to Figure 13. In addition, pressures calculated with FactSage™ 7.3 using the FactPS database are plotted. The equilibrium partial pressures of Ca, Mg, O and O_2 were calculated in the temperature range between 1800 and 2200 K for CaO and between 1600 and 2200 K for MgO. In these calculations, all possible gaseous reaction products were again taken into account. The partial pressures of O and O_2 above pure CaO are shown only beyond ~1873 K and those of O above pure MgO beyond ~1823 K because the ion intensity beneath these temperatures is very low and therefore the occurring fluctuations of the measured signal are very high, which causes high fluctuations of the calculated partial pressures.

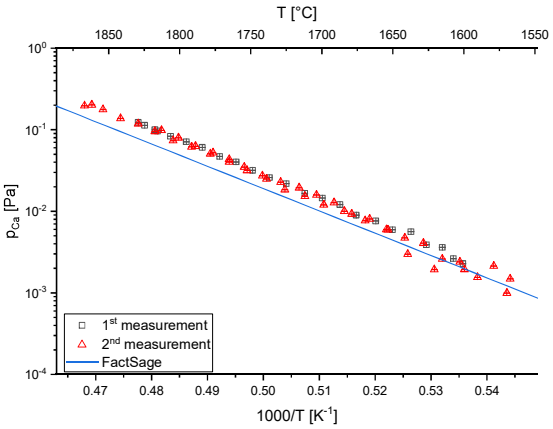

Figure 8: Temperature dependence of Ca vapor pressure above pure CaO

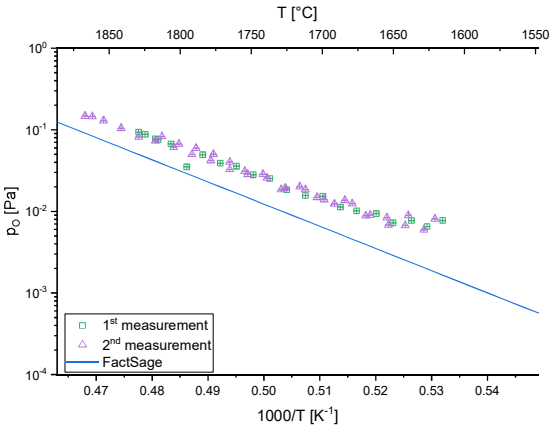

Figure 9: Temperature dependence of O vapor pressure above pure CaO

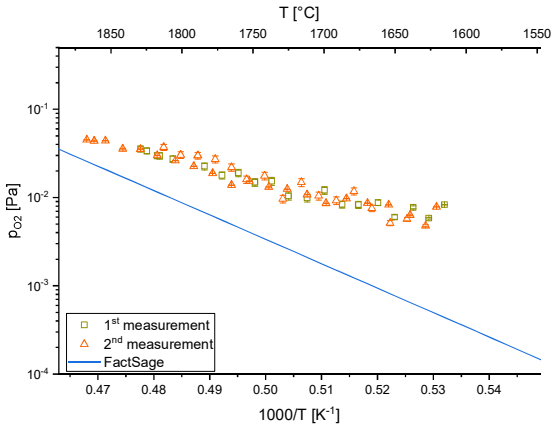

Figure 10: Temperature dependence of O_2 vapor pressure above pure CaO

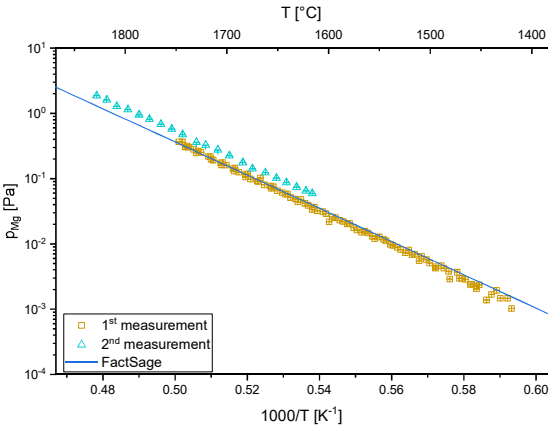

Figure 11: Temperature dependence of Mg vapor pressure above pure MgO

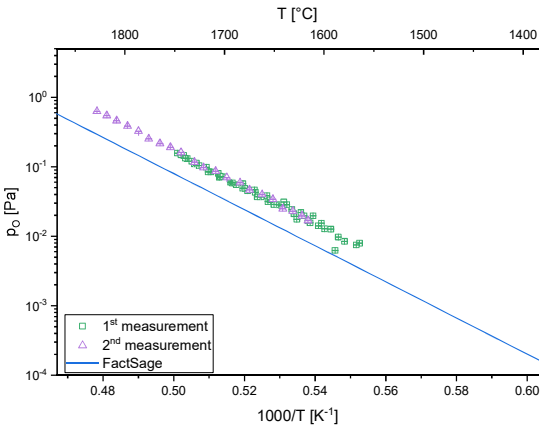

Figure 12: Temperature dependence of O vapor pressure above pure MgO

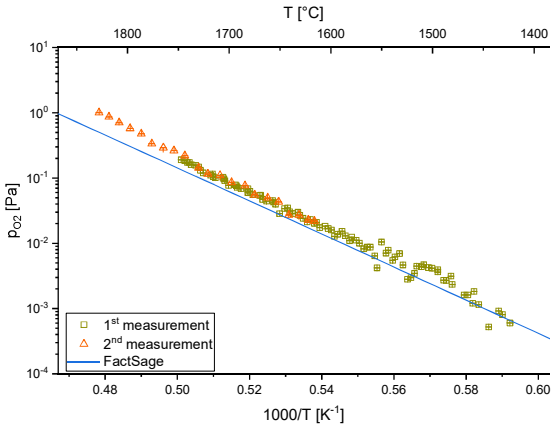

Figure 13: Temperature dependence of O_2 vapor pressure above pure MgO

As mentioned earlier in the isothermal experiments, errors can occur in the measurement of $^{16}O^+$ and $^{16}O_2^+$. To eliminate the influence of these possible measurement errors on the calculation of the reaction enthalpy, the partial pressures of O and O_2 are calculated from the determined Ca and Mg partial pressures, respectively. The equilibrium constants required for this at the relevant temperatures were calculated using FactSage™ and the FactPS database.

Assuming congruent, dissociative evaporation of CaO and MgO (Equation (13) and (14)) as well as recombination of atomic oxygen (Equation (15)), reaction Equations (16) and (17) result. Equations (18) and (19) represent the equilibrium constants for reactions (16) and (17), respectively. The activities of the pure substances (a_{CaO} und a_{MgO}) were set to 1. For better comparability with previous literature values, the sublimation enthalpies of calcium and magnesium were also considered, resulting in Equations (20) and (21).

$$CaO(s) \rightleftharpoons Ca(g) + O(g) \tag{13}$$

$$MgO(s) \rightleftharpoons Mg(g) + O(g) \tag{14}$$

$$2\,O(g) \rightleftharpoons O_2(g) \tag{15}$$

$$CaO(s) \rightleftharpoons Ca(g) + 0.5\,O_2(g) \tag{16}$$

$$MgO(s) \rightleftharpoons Mg(g) + 0.5\,O_2(g) \tag{17}$$

$$K_{CaO} = \frac{1}{p_{Ca} * \sqrt{p_{O_2}}} \tag{18}$$

$$K_{MgO} = \frac{1}{p_{Mg} * \sqrt{p_{O_2}}} \tag{19}$$

$$CaO(s) \rightleftharpoons Ca(s) + 0.5\,O_2(g) \tag{20}$$

$$MgO(s) \rightleftharpoons Mg(s) + 0.5\,O_2(g) \tag{21}$$

For the determination of the standard enthalpies of formation by the third law method, the Gibbs energy functions of all species involved were taken from the FactPS database. Table 4 compares the standard enthalpies of formation of this work along with those found in the literature. For the calculation of the enthalpy of formation, the vapor pressures of calcium below 1873 K were neglected due to the high fluctuations.

Table 4: Standard enthalpies of formation obtained by 3rd law method of CaO and MgO in comparison with literature

$\Delta_f H^\circ_{298}$ [kJ/mol]	Source	$\Delta_f H^\circ_{298}$ [kJ/mol]	Source
$Ca(s) + 0.5\ O_2(g) \rightleftharpoons CaO(s)$		$Mg(s) + 0.5\ O_2(g) \rightleftharpoons MgO(s)$	
-624±3	1st measurement	-604±4	1st measurement
-625±3	2nd measurement	-592±4	2nd measurement
-624.5±3.5	**mean**	**-598±10**	**mean**
-602±*3*	[9]	-635±*10*	[9]
-610±*4*	[3]	-589±15	[15]
-634±*1.5*	[4]	-601±1	[1]
-635±1	[1]	-601±*0.5*	[13]
-635±1	[11]	-602±*0.2*	[14]
-636	[12]	-602	[4]
-635	FactPS	-601	FactPS

Standard deviations of the determined values for $\Delta_f H^\circ_{298}$ are obtained considering the statistical deviation of the experimental data. The comparison of the standard enthalpies of formation of CaO determined by KEMS with available literature values (Table 4) shows a clear deviation. In the following, the procedure of the different researchers to determine the standard enthalpies of formation for CaO and MgO, which are listed in Table 4, is described and possible reasons for inaccuracies are pointed out.

A possible explanation for the deviation from the measured values of Gourishankar et al. in [9] is the experimental setup used. In the free evaporation experiments described in [9], the mass loss rate of CaO single crystals was determined in vacuum at a constant temperature. The temperature range was between 1919 and 2072 K. For the experiments, the researchers used an induction furnace in which the samples were hung on a molybdenum wire in the heating zone. The samples were heated by radiation from the graphite susceptor, which coupled to the induction field. The temperature was measured by an optical pyrometer. The pyrometer was calibrated by means of a type C thermocouple and measurement of the melting point of niobium oxide. According to Gourishankar et al, the pressure

inside the vacuum chamber never exceeded a pressure of $5 \cdot 10^{-4}$ Torr during the experiments. The researchers recorded the mass loss continuously using a Cahn electrobalance. They calculated the mass loss rates from the slopes of the mass loss time data recorded and the sample surface areas. They assumed that a fast surface reaction maintains the local equilibrium and that the gas transport from the near-surface region controls the mass loss. Only Ca(g), O(g), and O_2(g) species were considered in further calculations. All other species were considered as negligible under the experimental conditions. To calculate $\Delta_f H^\circ_{298,CaO}$, the researchers proceeded as follows. They started from the equilibria and the corresponding equilibrium constants K_i, which are shown in Equation (22) to (25).

$$0.5\ O_2(g) \rightleftharpoons O(g) \tag{22}$$

$$Ca(g) + 0.5\ O_2(g) \rightleftharpoons CaO(s) \tag{23}$$

$$K_O = \frac{p_O}{\sqrt{p_{O_2}}} \tag{24}$$

$$K_{CaO} = \frac{a_{CaO}}{p_{Ca}\sqrt{p_{O_2}}} \tag{25}$$

p_i represents the partial pressures of the respective species and a_{CaO} the activity of solid CaO, which was defined as 1. In addition, they used the Langmuir equation for an evaporation flux J_i, which is shown in Equation (26).

$$J_i = \frac{\alpha p_i}{\sqrt{2\pi M_i RT}} \tag{26}$$

α is an accommodation coefficient, which was set to 1 due to the assumed local equilibrium. M_i corresponds to the molar mass of the respective species, R and T are the universal gas constant and the temperature. Furthermore, Gourishankar et al. used the following equation (Equation (27)) for the mathematical expression of the mass loss rate $\dot{m}/A$:

$$\dot{m}/A = \frac{p_{Ca}\sqrt{M_{Ca}} + p_{O_2}\sqrt{M_{O_2}} + p_O\sqrt{M_O}}{\sqrt{2\pi RT}} \tag{27}$$

The researchers calculated K_{CaO} for each measured mass loss rate by incrementally changing the value of the equilibrium constant and thus the values of the partial pressures until the calculated mass loss rate was equal to the experimental one. Using the equilibrium constant obtained in this way, the free energy of formation for CaO $\Delta_f G^\circ_{T,CaO}$, which is calculated as shown in Equation (28), was computed.

$$\Delta_f G^\circ_{T,CaO} = -RT \ln K_{CaO} \quad (28)$$

293 In [9], the researchers calculated $\Delta_f H^\circ_{298,CaO}$ then finally as shown in Equation (29).

$$\Delta_f H^\circ_{298,CaO} = \Delta_f G^\circ_{T,CaO} - T\Delta(Gef)_{CaO} \quad (29)$$

294 They calculated $\Delta(Gef)_{CaO}$ from the Gibbs energy functions of the individual species $(Gef)_i$ contained in
295 Equation (23) as follows (Equation (30)):

$$\Delta(Gef)_{CaO} = (Gef)_{CaO(s)} - (Gef)_{Ca(ref.)} - 0.5(Gef)_{O_2(g)} \quad (30)$$

296 They took the Gibbs energy functions of the individual species from the 1985 JANAF tables. Using this procedure,
297 the researchers in [9] calculated $\Delta_f H^\circ_{298,CaO}$ for the measured mass loss rates of each of the six experiments. The
298 mean value of the results corresponds to -602 kJ/mol with a standard deviation of ±3 kJ/mol. A possible explanation
299 for the high mass loss rates measured by Gourishankar et al. in [9] and the resulting more positive value $\Delta_f H^\circ_{298,CaO}$,
300 compared to the value listed in the JANAF tables, could be the reaction between the CaO specimen and gaseous
301 carbon emitted from the graphite susceptor under the formation of CO. This assumption was also made by Jacob and
302 Varghese in [2].

303 Wakasugi et al. in [3] determined $\Delta_f H^\circ_{298,CaO}$ by equilibrating silver and a CaO-saturated slag in a graphite crucible
304 under an argon inert gas atmosphere with 10% CO in a temperature range from 1570 to 1831 K. To determine the
305 enthalpy of formation, the activity coefficient of calcium γ_{Ca} in silver was first determined by equilibrating a CaC_2-
306 saturated slag with silver in a graphite crucible under argon atmosphere in a temperature range from 1417 to 1832 K.
307 To calculate γ_{Ca} in silver, the researchers used in addition to the calcium content in the silver after the experiments
308 X_{Ca} also a relationship for the free energy of formation of solid CaC_2 $\Delta_f G^\circ_{CaC_2}$ from literature. This can be seen in
309 Equation (31).

$$\log \gamma_{Ca} = \frac{\Delta_f G^\circ_{CaC_2}}{2.30RT} - \log X_{Ca} \quad (31)$$

310 R and T are the universal gas constant and temperature. With the obtained activity coefficient, Wakasugi et al. in [3]
311 were able to determine the function of the free energy of formation (shown in Equation (32)) used to calculate the
312 standard enthalpy of formation.

$$\Delta_f G^\circ_{CaO} = RT(\ln \gamma_{Ca} + \ln X_{Ca} + \ln p_{CO}) \quad (32)$$

313 p_{CO} is the partial pressure of CO in the gas phase (0.1 atm). $\Delta_f H^{\circ}_{298,CaO}$ was calculated by the researchers in [3]
314 according to the third law method identical to Gourishankar et al. in [9] using Equation (29). They also assumed the
315 equilibrium shown in Equation (23) and used the Gibbs energy functions to calculate $\Delta(Gef)_{CaO}$ from the 1985
316 JANAF tables. Using this procedure, the researchers calculated $\Delta_f H^{\circ}_{298,CaO}$ for eight experiments. The mean value of
317 the results is 610 kJ/mol with a standard deviation of ±4 kJ/mol. Since in this publication of Wakasugi et al. no
318 information or reference to other publications was given how the gas composition was adjusted and controlled
319 during the experiments, how the sample material was heated and which method was used to determine the calcium
320 content in the silver, the reliability of the results obtained is reduced and reproducibility is impossible. Furthermore,
321 a standard deviation of ±21 kJ/mol for the free energy of formation of CaC_2 used is mentioned in [2], which in turn
322 affects the accuracy of the results.

323 Liang et al. in [4] modeled thermodynamic functions for crystalline CaO after critically reviewing the literature. The
324 researchers' model is based on the temperature T dependent function for the Gibbs energy of solid CaO $G^{0,s}_{CaO}(T)$
325 shown in Equation (33).

$$G^{0,s}_{CaO}(T) = A + BT + CT\ln T + DT^2 + ET^3 + F_1T^{-1} \quad (33)$$

326 The researchers accepted the parameters B, C, D, E and F_1 for the temperature range from 298 to 3222 K from
327 Huang et al. from [46]. The calculation of parameter A is based on $\Delta_f H^{\circ}_{298,CaO}$, which Liang et al. obtained by
328 critically reviewing the literature. After careful analysis of $\Delta_f H^{\circ}_{298,CaO}$ determined by Gourishankar et al. in [9],
329 Liang et al. rejected this value for their modeling. Critically reviewing the work of Huber and Holley [11] and
330 Rossini et al. [12], from which the value listed in the NIST-JANAF tables [1] resulted, the researchers in [4]
331 concluded a value for $\Delta_f H^{\circ}_{298,CaO}$ of -634±1.5 kJ/mol. Since this value is based on the two works which are also the
332 basis for that in [1], such a small deviation of 1 kJ/mol is foreseeable.

333 The value for $\Delta_f H^{\circ}_{298,CaO}$ in the NIST-JANAF tables [1] is based on only two experimental measurements. One was
334 the determination of the enthalpy of combustion of Ca by bomb calorimetry by Huber and Holley in [11] and the
335 second was acid solution calorimetry reported by Rossini et al. in [12]. The two values obtained for $\Delta_f H^{\circ}_{298,CaO}$
336 differ by only 0.07%. These values, as well as the concluded value, which is tabulated in [1], are largely assumed to
337 be correct. In the work of Huber and Holley, metallic calcium was burned in a bomb calorimeter at an oxygen
338 pressure of 50 atm. To consider the influence of impurities in the calcium metal when measuring the heat of

combustion, the content of metallic impurities was measured spectroscopically, that of nitrogen by the Kjedhal method, the content of oxygen and carbon by combustion, and that of oxygen by the method of Eberle, Lerner and Patretic [47]. Huber and Holley assumed that the oxygen dissolved in calcium is present as CaO, carbon as CaC_2, and hydrogen as CaH_2. Combining the measured contents of the impurities and assuming how they are present results in the composition shown in Table 5. This table also lists the heats of combustion Q_i of the different substances used in [11].

Table 5: Composition of the Ca sample and heats of combustion of the different species taken from [11]

Element/Compound	Content [wt.-%]	Q_i [J/g]
CaC_2	0.029	26970
CaH_2	0.52	18880
CaO	0.07	-
Mg	0.01	24670
Ca	99.37	?

From the calorimetric measurements, an average heat of combustion for the calcium samples of 15815.8 J/g was obtained. By converting Equation (34) to Q_{Ca}, Huber and Holley calculated the heat of combustion of pure calcium.

$$0.9937Q_{Ca} + 0.00029Q_{CaC_2} + 0.0052Q_{CaH_2} + 0.00010Q_{Mg} = 15816 \quad (34)$$

In [11], for Q_{Ca} 15806.5 J/g and for the resulting value of the reaction energy ΔE inside the calorimeter -633.52±0.89 kJ/mol is given. To calculate $\Delta_f H^\circ_{298,CaO}$ from ΔE, the two researchers corrected for the deviation of oxygen from the ideal gas law. This resulted in a value of $\Delta_f H^\circ_{298,CaO}$ of -635.09±0.89 kJ/mol. The standard deviation of the enthalpy of formation results from inaccuracies of the individual methods. The researchers state that the inaccuracy of determination of C and H content is 2% and that of Mg content is 50%. Furthermore, they report that the O content could be determined to within ±0.03%. The researchers interpreted these inaccuracies as a 0.1% uncertainty in the resulting heat of combustion of calcium by assuming the maximum contents of the impurities. The total uncertainty of 0.14% results from the 0.03% uncertainty in the determination of the calorimeter energy equivalent, the 0.09% uncertainty in the calorimetric measurements, and the 0.1% uncertainty in the correction for impurities mentioned above. Taking into account the data of Huber and Holley in [11] concerning the accuracy of each method and the use of all necessary data given in [11], $\Delta_f H^\circ_{298,CaO}$ was recalculated. The minimum contents of impurities were also included. The value of the recalculation is -635.18±1.23 kJ/mol. This value is

0.09 kJ/mol more negative than the value given in [11] and accepted in [1]. The value for $\Delta_f H^\circ_{298,CaO}$ published by Rossini et al. in [12] can be traced back to nine different solution calorimetry studies according to Liang et al. from [4], but only the value of the earliest publication from 1905 was tabulated as -635.55 kJ/mol. In [4], all nine original papers were analyzed in detail and a new value for $\Delta_f H^\circ_{298,CaO}$ was calculated from them. The reactions considered with the corresponding reaction enthalpies $\Delta_r H_i$ is shown in Table 6.

Table 6: Reactions with corresponding reaction enthalpies taken from [4]

Reaction number	Single Reactions	$\Delta_r H_i$ [kJ/mol]
1	$Ca(s) + 2HCl(aq) = CaCl_2(aq) + H_2(g)$	-542.77
2	$CaO(s) + 2HCl(aq) = CaCl_2(aq) + H_2O(l)$	-197.50
3	$H_2(g) + 0.5O_2(g) = H_2O(l)$	-285.83
	Total Reaction	
4	$Ca(s) + 0.5O_2(g) = CaO(s)$	-631.10

For $\Delta_r H_i$ of reactions 1 and 2, the researchers in [4] used the mean of what they considered to be plausible and reliable values from the original nine publications. That of reaction 3 was taken from the NIST-JANAF tables [1]. The enthalpy of reaction for reaction 4 which equals $\Delta_f H^\circ_{298,CaO}$ is calculated as shown in Equation (35).

$$\Delta_r H_{Reaction\,1} - \Delta_r H_{Reaction\,2} + \Delta_r H_{Reaction\,3} = \Delta_r H_{Reaction\,4} \tag{35}$$

The resulting value is 4.45 kJ/mol more positive than the value tabulated in [12] and accepted in [1]. A close review of the original work on the determination of $\Delta_f H^\circ_{298,CaO}$, shows deviations from that which is tabulated in [1]. This, in turn, gives reason to question the precision of this value.

For determining $\Delta_f H^\circ_{298,MgO}$ Gourishankar et al. in [9] performed free evaporation experiments with MgO single crystals as well as sintered polycrystalline MgO specimens in a temperature range between 1834 and 2053 K in the same way as with CaO. Based on the measured mass loss rates of the different sample types, the researchers concluded that they are independent of the structure (single crystal or polycrystal) of the samples. For the determination of the standard enthalpy of formation of MgO, they considered the equilibria shown in Equation (22) and (36) and the corresponding equilibrium constants (Equation (24) and (37)).

$$Mg(g) + 0.5\,O_2(g) \rightleftharpoons MgO(s) \tag{36}$$

$$K_{MgO} = \frac{a_{MgO}}{p_{Mg}\sqrt{p_{O_2}}} \tag{37}$$

p_{Mg} is the partial pressure of Mg in the gas phase and the activity of MgO a_{MgO} was set to 1 due to the assumed local equilibrium. The further procedure for the calculation of $\Delta_f H^\circ_{298,MgO}$ is identical to that of $\Delta_f H^\circ_{298,CaO}$, as described earlier. When calculating the individual quantities, of course, the partial pressure, equilibrium constant, free energy of formation, and Gibbs energy functions of MgO or Mg must be used instead of those of CaO or Ca. Gourishankar et al. took the Gibbs energy functions for MgO(s) and Mg(ref.) from the 1985 JANAF tables. The mean value of $\Delta_f H^\circ_{298,MgO}$ determined by the third law method from the sixteen experiments performed by the researchers is -635 kJ/mol with a standard deviation of ±10 kJ/mol. As previously mentioned in the experiments of Gourishankar et al. with CaO, a reaction between gaseous carbon and the sample material may have occurred forming CO. Furthermore, it could be possible that the molybdenum used for the suspension of the specimens led to the reduction of the MgO. This consideration is based on calculations by FactSage™ 7.3 using the FactPS database. However, the two reactions that may have occurred are not an explanation for the low mass loss rate measured and the consequent more negative standard enthalpy of formation determined by the researchers in [9], compared to the value tabulated in [1].

To investigate the evaporation behavior of MgO, Knudsen effusion experiments were carried out from Altman reported in [15]. For the experiments, the researcher used magnesium oxide crystals with a purity of 99.7% and Al_2O_3 as the cell material. The temperature during the experiments was monitored by an optical pyrometer, which was aligned with the effusion opening of the cell. The pyrometer was calibrated against a pyrometer calibrated by the National Bureau of Standards, by comparing the measured temperatures of both instruments when pointed at a tungsten lamp. Evaporation experiments were performed in a temperature range between 1884 and 2120 K. The partial pressures were calculated from the mass loss W of the samples after the experiments. For this purpose, Altman used Equation (38).

$$W = \frac{1.596 \cdot 10^{-5}}{\sqrt{T}} \sum_i p_i \sqrt{M_i} \tag{38}$$

p_i and M_i are the partial pressure and the molar mass of the effusing species and T corresponds to the temperature. The researcher considered the equilibrium shown in Equation (39) and the corresponding equilibrium constant (Equation (40)).

$$MgO(s) \rightleftharpoons Mg(g) + 0.5\ O_2(g) \tag{39}$$

$$K_{MgO} = \frac{p_{Mg}\sqrt{p_{O_2}}}{a_{MgO}} \tag{40}$$

Altman set the activity of MgO a_{MgO} 1. The combination of Equation (41) and (42) results in Equation (43) which, by substituting into Equation (38), finally allowed the researcher to calculate the partial pressure of magnesium from the measured mass losses of the seventeen experiments with the formula shown in Equation (44).

$$\sum_i p_i\sqrt{M_i} \rightleftharpoons p_{Mg}\sqrt{M_{Mg}} + p_{O_2}\sqrt{M_{O_2}} \tag{41}$$

$$\frac{p_{Mg}}{\sqrt{M_{Mg}}} = \frac{2p_{O_2}}{\sqrt{M_{O_2}}} \tag{42}$$

$$\sum_i p_i\sqrt{M_i} \rightleftharpoons p_{Mg}\left(\sqrt{M_{Mg}} + \frac{M_O}{\sqrt{M_{Mg}}}\right) = 8.18p_{Mg} \tag{43}$$

$$p_{Mg} = 7.66 \cdot 10^{-7}\sqrt{T}W \tag{44}$$

By using free energy functions from the literature and including the mass loss of the alumina Knudsen cells, the researcher in [15] determined an average value for $\Delta_f H^\circ_{298,MgO}$ of -589 kJ/mol with a standard deviation of ±15 kJ/mol. This value already takes into account the sublimation enthalpy of Mg. Altman also performed experiments with empty Al_2O_3 cells and reported in [15] that the weight losses of the empty cells were in the same order of magnitude as those of the cells with MgO. The small difference between the mass loss of the empty cells and those containing MgO suggests that the deviations in the measurement results are much larger than reported. Furthermore, the use of Al_2O_3 as cell material for the investigation of the evaporation behavior of MgO poses a major problem. Because spinel formation occurs and thus on the one hand the mass loss as well as the magnesium partial pressure calculated from it and $\Delta_f H^\circ_{298,MgO}$ are influenced. Altman reported in [15] that the determined p_{Mg} in experiments with $MgAl_2O_4$ as sample material differ from those calculated in experiments with MgO as sample material. This allows the assumption that not all MgO in the alumina cell reacted to spinel, but it does not exclude the spinel formation and thus the influence on the mass loss.

The value tabulated in the NIST-JANAF tables [1] for $\Delta_f H^\circ_{298,MgO}$ is based on the work of Holley and Huber in [13], who used bomb calorimetry to determine the enthalpy of combustion of metallic Mg, and Shomate and Huffman in [14], who used HCl solution calorimetry. Values of -601.23±0.49 kJ/mol and -601.83±0.21 kJ/mol for $\Delta_f H^\circ_{298,MgO}$ were obtained. These values differ from each other by only 0.1%.

In the work of Holley and Huber, reported in [13], the researchers burned doubly distilled magnesium with a purity of ≥99.98%. One of the major impurities was silicon, the content of which is reported to be ≤0.01%. The researchers additionally detected a nitrogen content in the magnesium of 0.004%. Holley and Huber performed fifteen experiments in total, where the mean combustion energy of magnesium Q_{Mg} was 24667±8 J/g. Including the uncertainty in the determination of the energy equivalence, a value of 24667±20 J/g resulted for Q_{Mg}. This combustion energy delivers a value of -599.90 kJ/mol for the reaction energy ΔE inside the calorimeter. To calculate $\Delta_f H^\circ_{298,MgO}$ of ΔE, the researchers in [13] proceeded identically to the determination of $\Delta_f H^\circ_{298,CaO}$ in [11] and also again corrected for the deviation of oxygen from the ideal gas law. This results in a value of -601.23±0.49 kJ/mol.

Shomate and Huffman determined in [14] $\Delta_f H^\circ_{298,MgO}$ by acid solution calorimetry with 1 N HCl. The researchers considered the reactions shown in Table 7 with the corresponding enthalpies of reaction $\Delta_r H_i$ and calculated the enthalpy of reaction of the total reaction which is equal to $\Delta_f H^\circ_{298,MgO}$.

Table 7: Reactions with corresponding reaction enthalpies taken from [14]

Reaction number	Single Reactions	$\Delta_r H_i$ [kJ/mol]
1	$Mg(s) + 2HCl(aq) = MgCl_2(aq) + H_2(g)$	-465.77±0.17
2	$CaO(s) + 2HCl(aq) = MgCl_2(aq) + H_2O(l)$	-149.78±0.09
3	$H_2(g) + 0.5O_2(g) = H_2O(l)$	-285.84±0.04
	Total Reaction	
4	$Mg(s) + 0.5O_2(g) = MgO(s)$	-601.83±0.21

$\Delta_r H_{Reaction\,1}$ is the average of six measurements and corrected for the vaporization of water by the resulting hydrogen. $\Delta_r H_{Reaction\,2}$ was calculated in [14] from five measurements and corrected for the heat of dilution caused by the water formed in Reaction 2. The researchers adopted $\Delta_r H_{Reaction\,3}$ from the literature [48]. $\Delta_r H_{Reaction\,4}$ respectively $\Delta_f H^\circ_{298,MgO}$ is obtained as shown in Equation (35). Since both the enthalpy of Reaction 1 and 2 were determined experimentally by Shomate and Huffman and the documentation of the procedure is plausible, the results seem reliable. Since in [13] as well as in [14] the determined values for $\Delta_f H^\circ_{298,MgO}$ are comprehensible, the correctness of the value tabulated in [1] can be assumed. Only the age of the publications leads to the conclusion that the accuracy of the methods used does not represent the current state of the art and therefore the deviations of the measurements should be assumed to be higher.

In [4], Liang et al. modeled not only the temperature-dependent Gibbs energy function for CaO, as already mentioned, but also that for MgO. The procedure was almost identical. The parameters A to F_1, shown in Equation (33), for the calculation of $G_{MgO}^{0,S}(T)$ in the temperature range 298-1700 K were taken from [46]. To compensate for a small jump in dC_p/dT at 1700 K, the researchers adjusted all the parameters in the temperature range between 1700 and 3250 K. Similarly, they adjusted parameters A and B in the temperature range of 3250-5000 K. This fitting required $\Delta_f H_{298,MgO}^{\circ}$. The value for the standard enthalpy of formation was adopted by the researchers from [1] after careful analysis of the experimental work. The value documented by Gourishankar et al. in [9] was rejected by the researchers. After the adjustment, the researchers were able to ensure the continuity conditions of the Gibbs energy, enthalpy, C_p, and dC_p/dT functions. The standard enthalpy of formation for MgO calculated from the fitted parameters has the value, reported by the researchers in [4], -601.60±1 kJ/mol. Since the parameter fit is based partly on $\Delta_f H_{298,MgO}^{\circ}$ from [1], the small negative deviation, from the value tabulated in [1], of 0.36 kJ/mol is foreseeable.

A major advantage of Knudsen effusion mass spectrometry compared to other methods for determining thermodynamic data is that with KEMS these are determined from the gas phase, which is in equilibrium with the condensed phase. This means that, in contrast to other methods involving the condensed phase, the influence of defects and impurities in the condensed phase on the results can be largely avoided. Many of the data tabulated in [1] are already based on KEMS measurements, which indicates the reliability and reproducibility of the measurement results of this method. Jacobson et al. in [26] gathered a collection of publications representing the wide range of possible applications of KEMS. Due to the mentioned possible inaccuracies of the literature values for $\Delta_f H_{298,CaO}^{\circ}$ and $\Delta_f H_{298,MgO}^{\circ}$ it can be assumed that the data determined in the course of this work are closer to reality than the values currently tabulated in [1].

Based on the results of the evaporation tests, the FactSage™ 7.3 calculations were adapted considering Ca, O and O_2 as gaseous products for the vaporization process of CaO. For the calculation of the MgO vaporization reaction, Mg, O and O_2 were chosen as the possible products. In Figure 14 and Figure 15, the results were obtained in this way, using the FactPS database ($\Delta_f H_{298,CaO}^{\circ}$= -635 kJ/mol; $\Delta_f H_{298,MgO}^{\circ}$= -601 kJ/mol), are compared with the calculations using the determined standard enthalpies of formation for CaO and MgO. Pressure ranges are established by the deviations of the enthalpies of formation ($\Delta_f H_{298,CaO,max}^{\circ}$= -621 kJ/mol from the first measurement;

469 $\Delta_f H^\circ_{298,CaO,min}$= -628 kJ/mol from the second measurement; $\Delta_f H^\circ_{298,MgO,max}$= -588 kJ/mol from the second

470 measurement; $\Delta_f H^\circ_{298,MgO,min}$= -608 kJ/mol from the first measurement). The calculations were also performed with

471 FactSage™ 7.3.

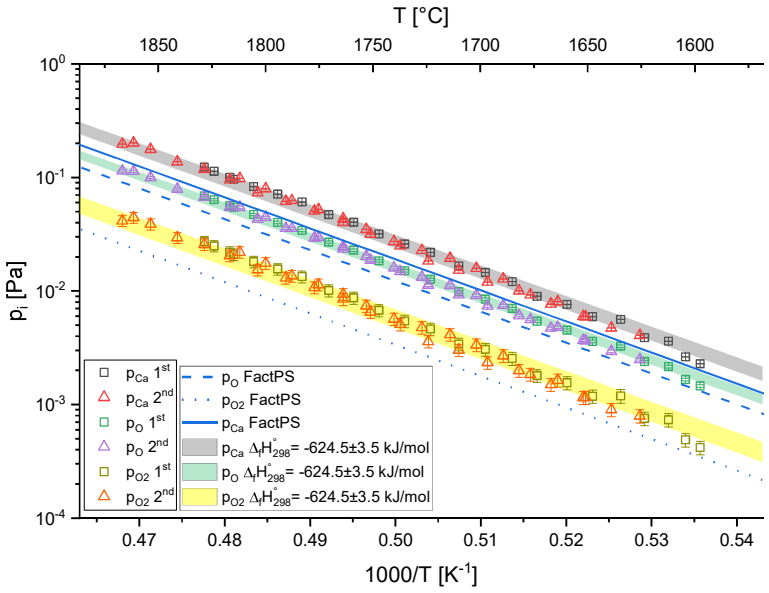

472

473 **Figure 14: Vapor pressures of gaseous species calculated with determined $\Delta_f H^\circ_{298,CaO}$**

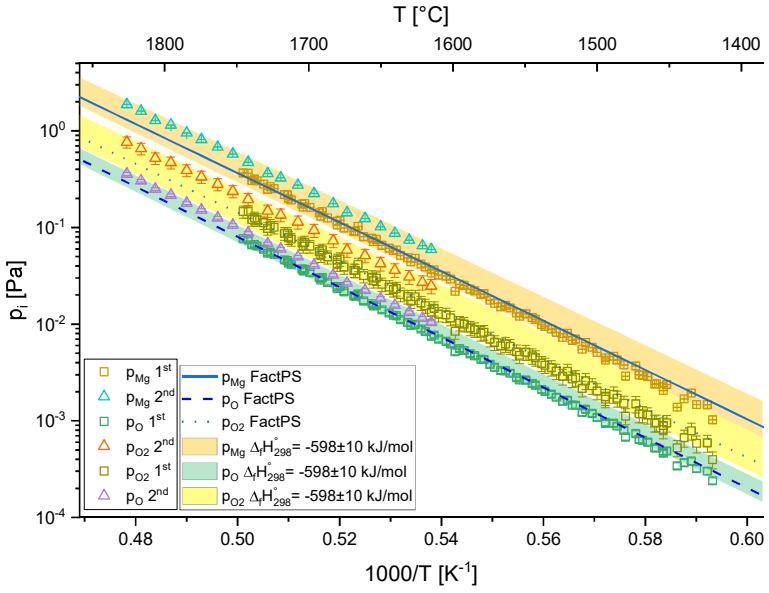

474

475 **Figure 15: Vapor pressures of gaseous species calculated with determined $\Delta_f H^\circ_{298,MgO}$**

In addition to the effects shown on the partial pressures of the different species, the implementation of these newly determined values for $\Delta_f H^\circ_{298,CaO}$ and $\Delta_f H^\circ_{298,MgO}$ in the FactSage™ databases would also have an impact on the calculated equilibria between different substances. Since the basis of the equilibrium calculations is the minimization of the Gibbs energy and the enthalpy of formation describes part of the Gibbs energy functions. Therefore, for example, as shown in Figure 16, the liquid slag region in the CaO-Al_2O_3-SiO_2-MgO system at 1600 °C would expand due to the lower thermodynamic stability of MgO and CaO. Also shown in this figure is the comparison with the result using the values for $\Delta_f H^\circ_{298,CaO}$ and $\Delta_f H^\circ_{298,MgO}$ stored in the FactPS and FToxid databases, respectively.

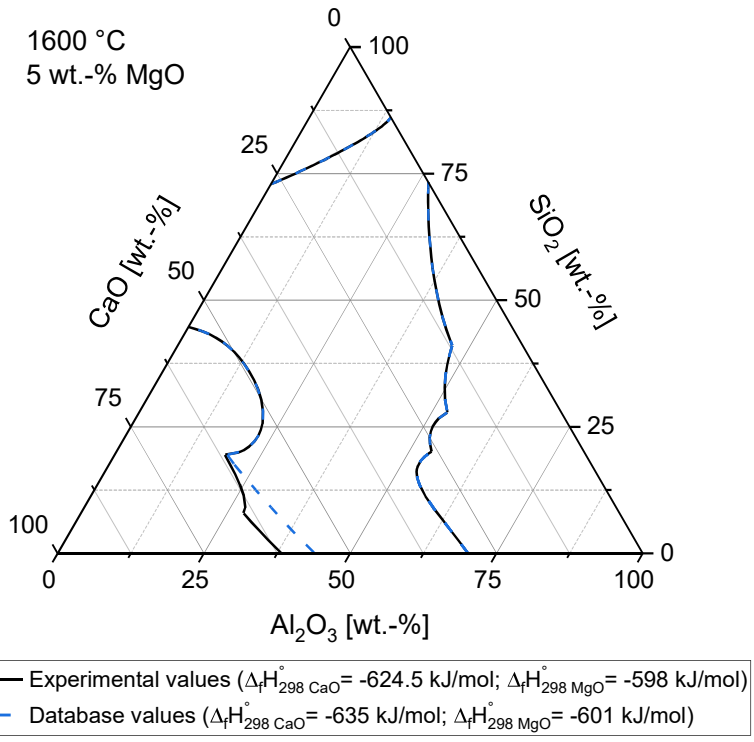

Figure 16: Impact of $\Delta_f H^\circ_{298,i}$ on the liquid slag region in the CaO-SiO_2-Al_2O_3-MgO system at 1600 °C

5. Conclusion

In the interest of future activity measurements, due to the high scatter of literature data, the thermodynamic properties of solid CaO and MgO were quantified using KEMS. The standard formation enthalpy of CaO of -624.5±3.5 kJ/mol determined in two different measurements can be considered as more reliable than the -635±1 listed in the NIST-JANAF in [1] tables. This rather large deviation of $\Delta_f H^\circ_{298,CaO}$ between the values determined by

KEMS and those listed in the NIST-JANAF tables [1] suggests that the values determined in this work are more consistent with performed experiments. For the standard enthalpy of formation of MgO, a value of -598±10 kJ/mol was determined in two measurements, which is only slightly more positive than the -601±1 kJ/mol listed in the NIST-JANAF tables [1]. Due to the very small deviation, the tabulated data can be considered to be correct, and the results obtained here can be used for further improvement of thermodynamic databases. However, the slight differences may be due to the selection of incorrect ionization cross sections, temperature calibration or variations in the Gibbs energy functions used.

6. Acknowledgments

The authors gratefully acknowledge the funding support of K1-MET GmbH, metallurgical competence center. The research programme of the K1-MET competence center is supported by COMET (Competence Center for Excellent Technologies), the Austrian programme for competence centers. COMET is funded by the Federal Ministry for Climate Action, Environment, Energy, Mobility, Innovation and Technology, the Federal Ministry for Labour and Economy, the Federal States of Upper Austria, Tyrol and Styria as well as the Styrian Business Promotion Agency (SFG) and the Standortagentur Tyrol. Furthermore, Upper Austrian Research GmbH continuously supports K1-MET. Beside the public funding from COMET, this research project is partially financed by the scientific partners Montanuniversitaet Leoben and University of Applied Sciences - Upper Austria and the industrial partners Lhoist Recherche et Développement SA, Primetals Technologies Austria GmbH, RHI Magnesita GmbH, voestalpine Stahl GmbH, and voestalpine Stahl Donawitz GmbH.

7. Conflict of Interest

On behalf of all authors, the corresponding author states that there is no conflict of interest.

8. References

1. Chase, Malcolm, W., Jr.: *Journal of Physical and Chemical Reference Data: NIST-JANAF thermochemical tables,* 4th ed., American Chemical Society and American Institute of Physics, Woodbury, NY, 1998.
2. K. T. Jacob and V. Varghese: *Metallurgical and Materials Transactions B*, 1996, vol. 27, pp. 647–51.
3. T. Wakasugi and N. Sano: *Metallurgical and Materials Transactions B*, 1989, vol. 20, pp. 431–33.
4. S.-M. Liang, A. Kozlov, and R. Schmid-Fetzer: *International Journal of Materials Research*, 2018, vol. 109, pp. 185–200.

5. Q. Wen, F. Shen, H. Zheng, J. Yu, X. Jiang, and Q. Gao: *ISIJ International*, 2018, vol. 58, pp. 792–98.

6. G. Deffrennes, N. Jakse, C. M. Alvares, I. Nuta, A. Pasturel, A. Khvan, and A. Pisch: *Calphad*, 2020, vol. 69, p. 101764.

7. L. B. Pankratz: *Thermodynamic Properties of Elements and Oxides,* United States Department of Interior, Washington DC, 1982.

8. I. Barin, O. Knacke, and O. Kubaschewski: *Thermochemical properties of inorganic substances: Supplement,* Springer Berlin Heidelberg, Berlin, Heidelberg, 1977.

9. K. V. Gourishankar, M. K. Ranjbar, and G. R. St. Pierre: *Journal of Phase Equilibria*, 1993, vol. 14, pp. 601–11.

10. M. Miller and K. Armatys: *The Open Thermodynamics Journal*, 2013, vol. 7, pp. 2–9.

11. E. J. Huber and C. E. Holley: *The Journal of Physical Chemistry*, 1956, vol. 60, pp. 498–99.

12. F. D. Rossini, D. D. Wagman, W. H. Evans, S. Levine, and I. Jaffe: *Selected Values of Chemical Thermodynamic Properties,* U.S. Government Printing Office, Washington, D.C., 1952.

13. C. E. Holley and E. J. Huber: *Journal of the American Chemical Society*, 1951, vol. 73, pp. 5577–79.

14. C. H. Shomate and E. H. Huffman: *Journal of the American Chemical Society*, 1943, vol. 65, pp. 1625–29.

15. R. L. Altman: *The Journal of Physical Chemistry*, 1963, vol. 67, pp. 366–69.

16. M. Hillert: *Physica B+C*, 1981, vol. 103, pp. 31–40.

17. C. W. Bale, P. Chartrand, S. A. Degterov, G. Eriksson, K. Hack, R. Ben Mahfoud, J. Melançon, A. D. Pelton, and S. Petersen: *Calphad*, 2002, vol. 26, pp. 189–228.

18. P. F. Shi, A. Engström, B. Sundman, and J. Ågren: *Materials Science Forum*, 2011, 675-677, pp. 961–74.

19. D. Sergeev, E. Yazhenskikh, D. Kobertz, and M. Müller: *Calphad*, 2019, vol. 65, pp. 42–49.

20. Z. H. Dong, D. Sergeev, D. Kobertz, N. D'Souza, S. Feng, M. Müller, and H. B. Dong: *Metallurgical and Materials Transactions A*, 2020, vol. 51, pp. 309–22.

21. D. Spathara, D. Sergeev, D. Kobertz, M. Müller, D. Putman, and N. Warnken: *Journal of Alloys and Compounds*, 2021, vol. 870, p. 159295.

22. M. Heyrman, I. Nuta, and C. Chatillon: *Miscellaneous Methods and Applications of Elemental MS*, 2010, pp. 717–29.

23. K. Hilpert: *Rapid Communications in Mass Spectrometry*, 1991, vol. 5, pp. 175–87.

24. D. Kobertz, M. Müller, and A. Molak: *Calphad*, 2014, vol. 46, pp. 62–79.

25. D. Kobertz: *The Open Thermodynamics Journal*, 2013, vol. 7, pp. 71–76.

26. N. Jacobson, D. Kobertz, and D. Sergeev: *Calphad*, 2019, vol. 65, pp. 111–26.

27. K. Hilpert: *Noble Gas and High Temperature Chemistry. Structure and Bonding*, pp. 97–198.

28. G. R. Belton and R. J. Fruehan: *The Journal of Physical Chemistry*, 1967, vol. 71, pp. 1403–09.

29. D. Raj, L. Bencze, D. Kath, W. A. Oates, J. Herrmann, L. Singheiser, and K. Hilpert: *Intermetallics*, 2003, vol. 11, pp. 1119–24.

30. A. Neckel and S. Wagner: *Berichte der Bunsengesellschaft*, 1969, vol. 2, pp. 210–17.

31. L. Bencze, M. Ryś-Matejczuk, E. Yazhenskikh, M. Ziegner, and M. Müller: *Energy & Fuels*, 2016, vol. 30, pp. 657–65.

32. L. Bischof, P. A. Sossi, D. Sergeev, M. Müller, and M. W. Schmidt: *Calphad*, 2023, vol. 80, p. 102507.

33. J. Drowart and P. Goldfinger: *Angewandte Chemie International Edition in English*, 1967, vol. 6, pp. 581–96.

34. E. H. Copland and N. S. Jacobson: *Mass Spectrometry Handbook*, pp. 1143–80.

35. T. Babeliowsky, A. Boerboom, and J. Kistemaker: *Physica*, 1962, vol. 28, pp. 1155–59.

36. K. Nakajima: *Mass spectrometry (Tokyo, Japan)*, 2016, vol. 5, S0055.

37. J. Drowart, C. Chatillon, J. Hastie, and D. Bonnell: *Pure and Applied Chemistry*, 2005, vol. 77, pp. 683–737.

38. I. Barin: *Thermochemical data of pure substances,* VCH, Weinheim, New York, 1995.

39. C. B. Alcock, V. P. Itkin, and M. K. Horrigan: *Canadian Metallurgical Quarterly*, 1984, vol. 23, pp. 309–13.

40. J. B. Mann: *Proceedings of the Conference on Mass Spectrometry*, University Park Press, Baltimore, 1970, pp. 814–19.

41. M. Monroe: *Molecular Weight Calculator*, 2014.

42. W. Lotz: *Zeitschrift fr Physik*, 1968, vol. 216, pp. 241–47.

43. H. Deutsch, K. Becker, M. Probst, and T. D. Märk: *Advances in Atomic Molecular and Optical Physics*, Elsevier, 2009, pp. 87–155.

44. D. Margreiter, H. Deutsch, and T. D. Märk: *International Journal of Mass Spectrometry and Ion Processes*, 1994, vol. 139, pp. 127–39.

45. R. S. Freund, R. C. Wetzel, R. J. Shul, and T. R. Hayes: *Physical review. A, Atomic, molecular, and optical physics*, 1990, vol. 41, pp. 3575–95.

46. W. Huang, M. Hillert, and X. Wang: *Metallurgical and Materials Transactions A*, 1995, vol. 26, pp. 2293–310.

47. A. R. Eberle, M. W. Lerner, and G. J. Petretic: *Analytical Chemistry*, 1955, vol. 27, pp. 1431–33.

48. F. D. Rossini: *Journal of Research of the National Bureau of Standards*, 1939, vol. 22, p. 407.